

Temperature sensitivity of GaN/AlN Quantum-Dot Semiconductor Optical Amplifiers (QD SOA)

Falah H. Al-Asadi

Physics Department, Science college, Thi-Qar University,
Nassiriya, Iraq.
e-mail: drfh24@yahoo.com

Abstract

Temperature sensitivity of GaN quantum dot (QD) is studied in detail in this paper. Non-Markovian gain, spontaneous emission, noise figure, small signal gain and output power are calculated at different temperatures ($T = 0, 200, 300, 400$ and 500) $^{\circ}\text{K}$.

Keyword: Temperature sensitivity, Quantum Dot (QD), Semiconductor Optical Amplifier (SOA), Non-Markovian gain, Rate equations (REs), Noise Figure.

I. Introduction

GaN is a wide-gap semiconductor that is usually crystallizes in the wurtzite lattice type (also known as hexagonal). However, it has been known since the early 1970's that the energy gap of wurtzite GaN is about 3.5 eV. While the first measured temperature dependence of the GaN energy gap yields Varshni

coefficients with signs opposite from those of the other III-V materials, subsequent investigations achieved good fits with conventional signs for α and β . The temperature dependence of the energy gap using the commonly employed Varshni formula [1] is given by

$$E_g(T) = E_g(T=0) - \frac{\gamma T^2}{T + \beta} \quad (1)$$

The parameters described above are generally sufficient to describe the conduction and valence band structures of nitride materials [1]. When the active region of the semiconductor optical amplifier (SOA) becomes in the form of quantum dots (QD), where energy states becomes completely quantized, a superior characteristics are expected to be obtained from this QD-SOA. Akiyama et al. defined an active layer containing quantum structure which amplifies light propagation [2]. Now it is confirmed that different methods can be used to fabricate QD devices, see for example the patents EP2320257A2 [3], US7935388 [4], US7881091 [5].

II. Gain of QDs

We calculated energy gap at different temperatures for GaN by the relation [6]

$$E_g(T) = 3.503 - 5.08 \times 10^{-4} \frac{T^2}{996 - T} \quad (2)$$

GaN dots are assumed to be in the form of cubes with (10×10×10) nm size for each dimension. Using quantum box model, we calculate QD energy levels in both conduction and valence band. Non-Markovian optical gain of QD structure is then calculated from the relation [7]

$$g(w) = \frac{2w\mu c}{Vn_r} \int \frac{\text{Re } \Xi(0, \Delta_{nml})}{1 - \text{Re } q_1(0)} |\hat{\epsilon} \cdot \mathbf{M}_{cv}|^2 [1 + \text{Re } g_2(\infty, \Delta_{nml})] [f_c - f_v] \delta(E_{cv} - E_{cnml} - E_{vnml} - E_g) dE_{cv} \quad (3)$$

Where w is the angular frequency of light, n_r is the refractive index of GaN, f_c and f_v are the Fermi functions, E_{cv} is the transition energy between nml conduction subband and same nml valence subband, and V is the volume of the QD. Both TE and TM momentum matrix elements of QDs are calculated by [8]

$$|\hat{x} \cdot \mathbf{M}_{cv}|^2 = \left(\frac{q\hbar}{2E_{cv}} \right)^2 \frac{1}{m_0} \left(\frac{m_0}{m_e^\Pi} - 1 \right) \cdot \frac{E_g [(E_g + \Delta_1 + \Delta_2)(E_g + 2\Delta_2) - 2\Delta_3^2]}{(E_g + \Delta_1 + \Delta_2)(E_g + \Delta_2) - \Delta_3^2} \quad (4)$$

$$|\hat{z} \cdot \mathbf{M}_{cv}|^2 = \left(\frac{q\hbar}{2E_{cv}} \right)^2 \frac{1}{m_0} \left(\frac{m_0}{m_e^\perp} - 1 \right) \cdot \frac{[(E_g + \Delta_1 + \Delta_2)(E_g + 2\Delta_2) - 2\Delta_3^2]}{(E_g + 2\Delta_2)} \quad (5)$$

The rate of spontaneous emission $r_{sp}(w)$ is calculated from [6]

$$r_{sp}(\hbar w) = \frac{8\pi n_r^2 (\hbar w)^2}{h^3 c^2} g_{sp}(\hbar w) \quad (6)$$

Where the spontaneous emission g_{sp} have the following contributions [9]

$$g_{sp}(\hbar w) = \left[\frac{2g_{sp}^{TE}(\hbar w) + g_{sp}^{TM}(\hbar w)}{3} \right] \quad (7)$$

In the non-Markovian, the spontaneous emission g_{sp} for the QD can be written as

$$g_{sp}^{\alpha}(\hbar\omega) = \frac{e^2}{n_r c \epsilon_o m_o^2 \omega} \int \frac{\text{Re} \Xi(0, \Delta_{nml})}{1 - \text{Re} q_1(0)} \left| \hat{\epsilon} \cdot \mathbf{M}_{cv}^{\alpha} \right|^2 \cdot [1 + \text{Re} g_2(\infty, \Delta_{nml})] [f_c(1 - f_v)] \delta(E_{cv} - E_{cnml} - E_{vnml} - E_g) dE_{cv} \quad (8)$$

$$\frac{\partial N_w}{\partial t} = \frac{J}{qL_w} - \frac{N_w(1 - f_{ES})}{\tau_{w2}} + \frac{N_w f_{ES}}{\tau_{2w}} - \frac{N_w}{\tau_{wR}} \quad (9)$$

Where Ξ refers to the momentum matrix elements for TE or TM polarizations. Also we calculated the spontaneous emission power spectrum $P_{spont}(\omega)$ by multiplying Eq.(6) by the optical energy $\hbar\omega$.

III. QD-SOA

Based on the rate equations [10] for the wetting layer (WL) carrier density N_w , occupation probabilities for ground and excited states (f and f_{ES}), respectively one can write

$$\frac{\partial f_{ES}}{\partial t} = \frac{N_w L_w (1 - f_{ES})}{N_Q \tau_{w2}} - \frac{N_w L_w f_{ES}}{N_Q \tau_{2w}} - \frac{(1 - f) f_{ES}}{\tau_{12}} + \frac{f(1 - f_{ES})}{\tau_{21}} \quad (10)$$

$$\frac{\partial f}{\partial t} = \frac{(1 - f) f_{ES}}{\tau_{21}} - \frac{f(1 - f_{ES})}{\tau_{12}} - \frac{f^2}{\tau_{1R}} - \frac{g_p L_{21}}{N_Q} (2f - 1) S_{av} \frac{\tau_{12}}{c \sqrt{\epsilon_s}} \Gamma \quad (11)$$

Note that, the relation between the carrier density in the QD ground state (N) and the carrier occupation probability f in the QD ground state is $f = N/2(N_Q/w_x)$

and w_x is the quantum box size. The average signal photon density S_{av} is given by [11]

$$S_{av} = \left[\frac{(G - 1)(1 - R_f)(1 + R_b G)}{(1 - \sqrt{R_f R_b G})^2 + 4 \sqrt{R_f R_b G} \sin \Phi} \right] \frac{P_{in} n_g}{\hbar \omega_p L_w D L_g} \quad (12)$$

Where P_{in} is the input signal power, n_g is the group refractive index, \hbar is the normalized Planck's constant, ω_p is the peak frequency, D is the width of the active layer, L is the cavity length,

g_p is the peak material gain, c is the free space light speed. Note that, the Fibry-Perot amplifier gain G is given by [12]

$$G = \frac{(1 - R_f)(1 - R_b)G_s}{(1 - \sqrt{R_f R_b} G_s)^2 + 4\sqrt{R_f R_b} G_s \sin^2 \Phi} \quad (13)$$

Where R_f the front mirror reflectivity, R_b the back mirror reflectivity. Φ is the phase angle while G_s is the single-pass gain of the structure, given by

$$G_s = \exp[(g_p \Gamma - \alpha_{int})L] \quad (14)$$

Where α_{int} is the loss coefficient. The carrier dynamics described by the rate equations are related only to electrons in the conduction band, the hole dynamics can be neglected due to their larger effective mass [10].

The noise figure is calculated with shot noise part from the relation [12]

$$F_n = 2n_{sp}(G-1)/G + (1/G) \quad (15)$$

The parameter n_{sp} is the spontaneous emission factor given by [13]

$$n_{sp} = \frac{\Gamma r_{spont}(\hbar\omega)}{[\Gamma g(\omega)] - \alpha_{int}} \quad (16)$$

Where $g(\omega)$ is the gain, Eq. (1), and $r_{spont}(\omega)$ is the rate of spontaneous emission calculated from Eq. (6).

IV. Results and Discussion

Energy gap is calculated for GaN at different temperatures. Then, QD energy levels are calculated using quantum box model using the parameters listed in Table (1). Non-Markovian gain is then calculated for this QD structure.

Fig. (1) Shows the non-Markovian gain for lattice temperatures ($T = 200, 300, 400, 500$ and 600 °K) where the gain increases with decreasing lattice temperature as it is expected. The peak gain wavelength is shifted to longer one with increasing temperature. The interesting point here is the wavelength shift (>60 nm) when the temperature increases from 200-600 K. Fig. (2)

shows the peak gain versus carrier density. A maximum point is appear in the curves. The peak for 600 K appears faster than coldest ones. This can be attributed to the population of the dots at these temperatures which becomes approximately random at 600K [14]. The ratio of TE/TM gain polarizations is shown in Fig. (3) which shown the same response for both polarizations this have an importance in some SOA applications. Fig. (4) shows the spectra of spontaneously emitted power where it is shown that the power reduced at high temperature.

Rate Equations model are solved at steady state case to address other SOA characteristics using the expression of the average signal photon density S_{av} , Eq. (12), and typical values of the material parameters listed in Table (2). Fig. (5) shows the small-signal gain for the temperatures addressed. Fig. (6) shows the small-signal gain versus current where the curves shows a maximum value as it is seen by gain-current curves. But the maximum value for $T=600K$ is shifted to appear earlier which can be reasoned to the same reson of Fig. (2). Fig. (7) shows the noise figure spectra at the studied temperatures. This SOA shows a low noise figure which can be distributed along spectrum of wavelengths (310-380nm). The noise figure-current curve is shown in Fig. (8) where the noise caches a constant value except the case of $T=600K$. Fig. (9) shows the output power versus current curve which gives a high power at $T=200K$ due to its high gain and low noise. The characteristics of this amplifier are summarized in Tables (3) and (4).

Conclusions

AIN QD SOA characteristics are addressed at different temperatures. Gain is calculated using non-Markovian model. Then the rate equations model is used to study other SOA characteristics. It is shown that gain, spontaneous emission power are reduced and the peak is shifted to longer wavelength with temperatures. A maximum point for gain-current curve is shifted at high temperature due to random population effect. This SOA shows a low noise figure and polarization independent.

References

- [1] I. Vurgaftman and J. R. Meyer, "Band parameters for nitrogen-containing semiconductors" J. of Appl. Phys., Vol. 94, No. 6, 2003.
- [2] Akiyama, T.: US20070091419A1 (2007).
- [3] EP2320257A2 Anti-reflection coated quantum dot resonator for wavelength division multiplexing optical communication.

- [4] US7935388 Process for forming a quantum-dot particle layer on a substrate.
- [5] US7881091 Methods of making quantum dot films.
- [6] W. Fang and S. L. Chuang, "Theoretical of GaN lasing and temperature sensitivity" J. of Appl. Phys. Lett. Vol. 67, No. 6, 1995.
- [7] D. Ahn, "Optical Gain of Quantum-Well Laser with non-Markovian Relaxation and Many-Body Effects" IEEE J. of Quantum Electronics, vol. 32, No. 6, June 1996.
- [8] A. P. Abiyasa, S. F. Yu, W. J. Fan, and S. P. Lau, "Theoretical investigation of excitonic gain in ZnO-MgxZn1-xO strained quantum wells", IEEE J. Quantum Electronics, 42,455-463, May 2006.
- [9] R. A. Arif, H. Zhao, Y. Khoon Ee, and N. Tansu, "Spontaneous emission and characteristics of staggered InGaN quantum-well light-emitting diodes" IEEE J. Quantum Electronics, 44, 573-580, 2008.
- [10] Y. Ben-Ezra, M. Haridim, and B. I. Lembrikov, "Theoretical analysis of gain-recovery time and chirp in QD-SOA", IEEE J. Quantum Electronics, 17, 9, 2005.
- [11] M. Vasileiadis, D. Alexandropoulos, M. J. Adams, H. Simos and D. Syvridis, "Potential of InGaAs/GaAs Quantum Dots for Applications in Vertical Cavity Semiconductor Optical Amplifiers" IEEE J. of Selected Topics in Quantum Electronics, vol. 14, No. 4, 2008.
- [12] E. Forestieri, "Optical Communication Theory and Techniques" Ch. 8, Springer, Pisa, Italy, 2005.
- [13] K. Komori, S. Arai and Y. Suematsu, "Noise Study of Low-Dimensional Quantum-Well Semiconductor Laser Amplifiers" IEEE J. Quantum Electronics, 28, pp. 1894-1900, 1992.
- [14] Ian O'Driscoll, Peter Blood and Peter M. Smowton, "Random Population of Quantum Dots in InAs–GaAs Laser Structures", IEEE J. Quantum Electronics, 46, pp. 525-532, 2010.

Tables:

Table 1: Parameters for wurtzite nitride binaries [1]

| Parameters | GaN | AlN |
|----------------------------|-------|--------|
| $E_g(\text{eV})$ | - | 6.25 |
| $\epsilon_{cr}(\text{eV})$ | 0.010 | -0.169 |
| $\epsilon_{so}(\text{eV})$ | 0.017 | 0.019 |
| m_e | 0.20 | 0.32 |
| m_h | 0.20 | 0.30 |
| A_1 | -7.21 | -3.86 |
| A_2 | -0.44 | -0.25 |
| A_3 | 6.68 | 3.58 |
| A_4 | -3.46 | -1.32 |
| A_5 | -3.40 | -1.47 |

| | | |
|-------|-------|-------|
| A_6 | -4.90 | -1.64 |
| n_r | 3.1 | |

Table (2) : Parameters used in the Calculations.

| Parameter | Value | Unit |
|-------------|--------------------|------------------|
| L | 200 | μm |
| L_w | 0.2 | μm |
| D | 10 | μm |
| N_Q | 5×10^{12} | cm^{-2} |
| w_2 | 3 | ps |
| $2w$ | 1 | ns |
| l_2 | 1.2 | ps |
| $2l$ | 0.16 | ps |
| $1R$ | 0.4 | ns |
| wR | 1 | ns |
| | 0 | |
| $R_f = R_b$ | 10^{-4} | |
| int | 3 | 1/cm |
| | 0.006 | |
| L_b | 20 | nm |
| L_c | 75 | nm |
| P_{in} | 1 | μW |

Table (3) : Values of gain, small signal gain and noise figure at the peak wavelength.

| Temperatures (k) | Non- Markovian gain (1/cm) | Gain (dB) | Noise Figure (dB) | Peak wavelength (nm) |
|---------------------|----------------------------------|-----------|----------------------|----------------------------|
| 200 | 44055.83 | 22.86164 | 2.721206 | 0.31759 |
| 300 | 38235.03 | 19.74567 | 2.768726 | 0.32086 |
| 400 | 32810.12 | 16.87971 | 2.883035 | 0.32673 |
| 500 | 30182.5 | 15.49892 | 3.055966 | 0.33733 |
| 600 | 27835.77 | 14.26838 | 4.109921 | 0.38002 |

Table (4) : Values output power for different temperatures at input power $1\mu\text{W}$ and $(2 \times 10^{25} \text{ m}^{-3})$

| Temperatures (k) | Output power (W) |
|------------------|--------------------------|
| 200 | 1.93230×10^{-4} |
| 300 | 3.97562×10^{-5} |

| | |
|-----|---------------------------|
| 400 | 5.41157×10^{-5} |
| 500 | 3.547217×10^{-5} |
| 600 | 2.672008×10^{-5} |

Figures:

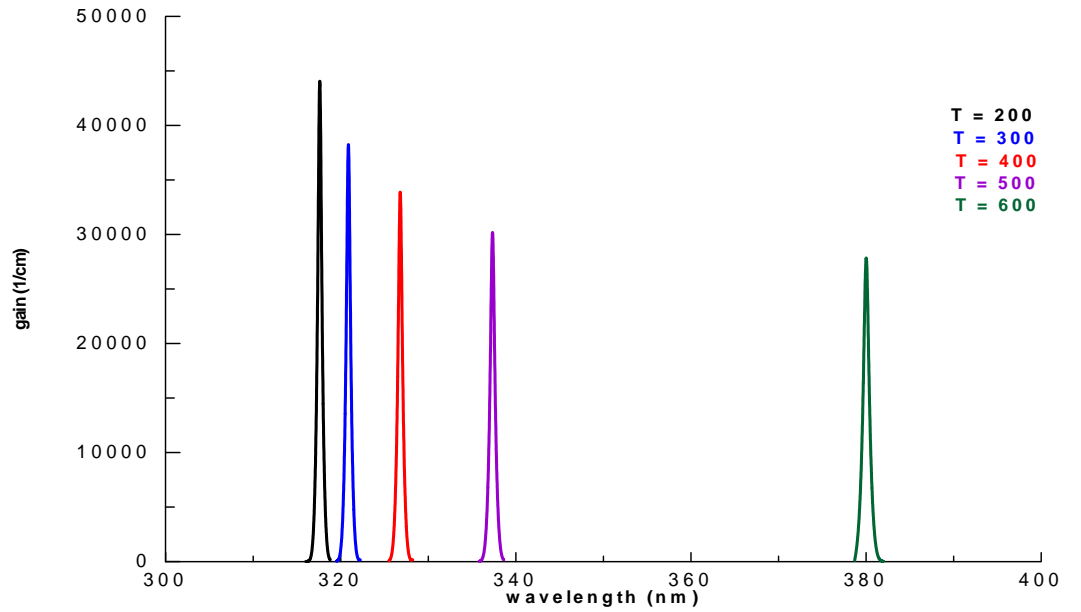


Fig. (1): Non-Markovian gain versus wavelength for temperatures ($T = 200, 300, 400, 500$ and 600).

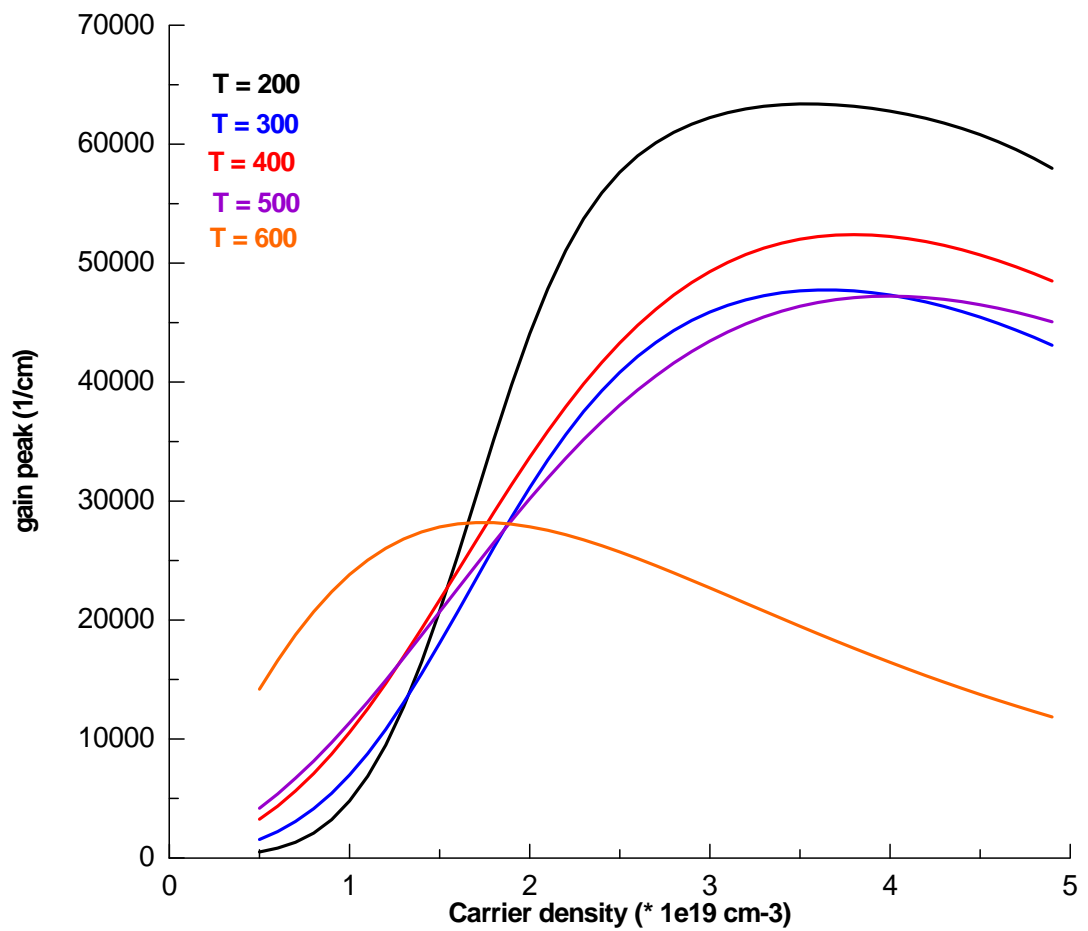


Fig. (2): Peak gain versus carrier density for temperatures ($T = 200, 300, 400, 500$ and 600).

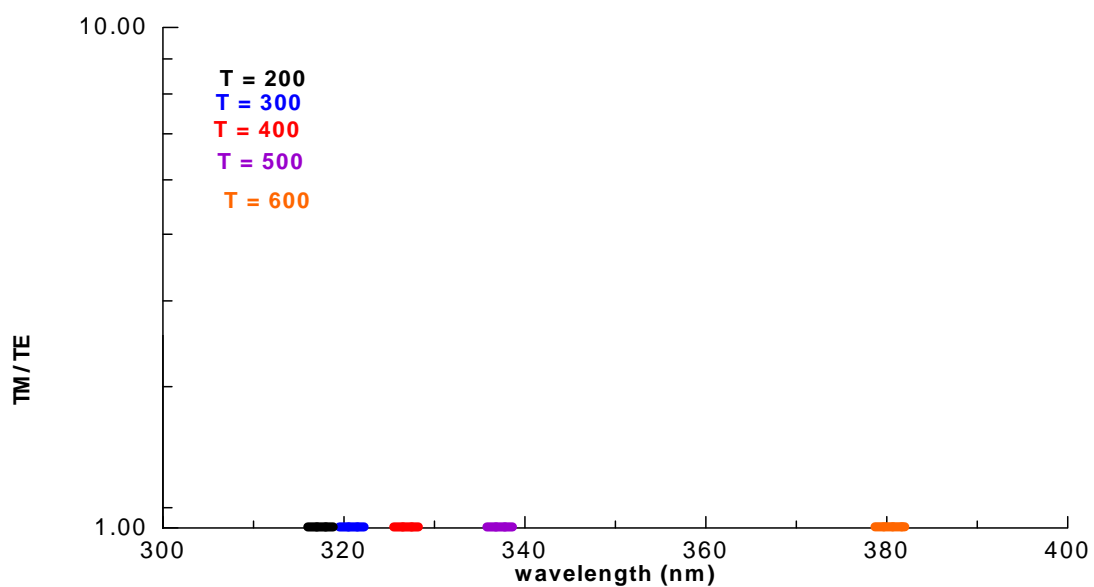


Fig. (3): TM/TE ratio at temperatures ($T = 200, 300, 400, 500$ and 600).

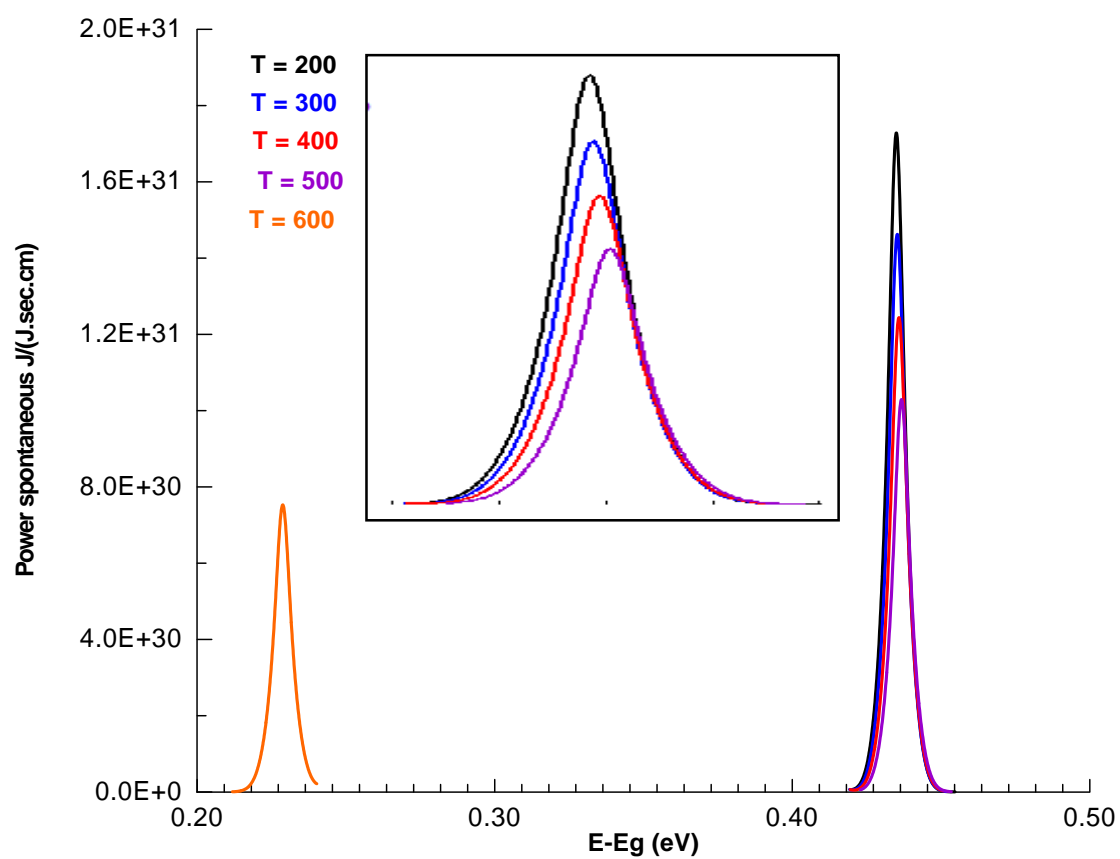


Fig. (4): spontaneous emission Power versus energy for temperatures ($T = 200, 300, 400, 500$ and 600).

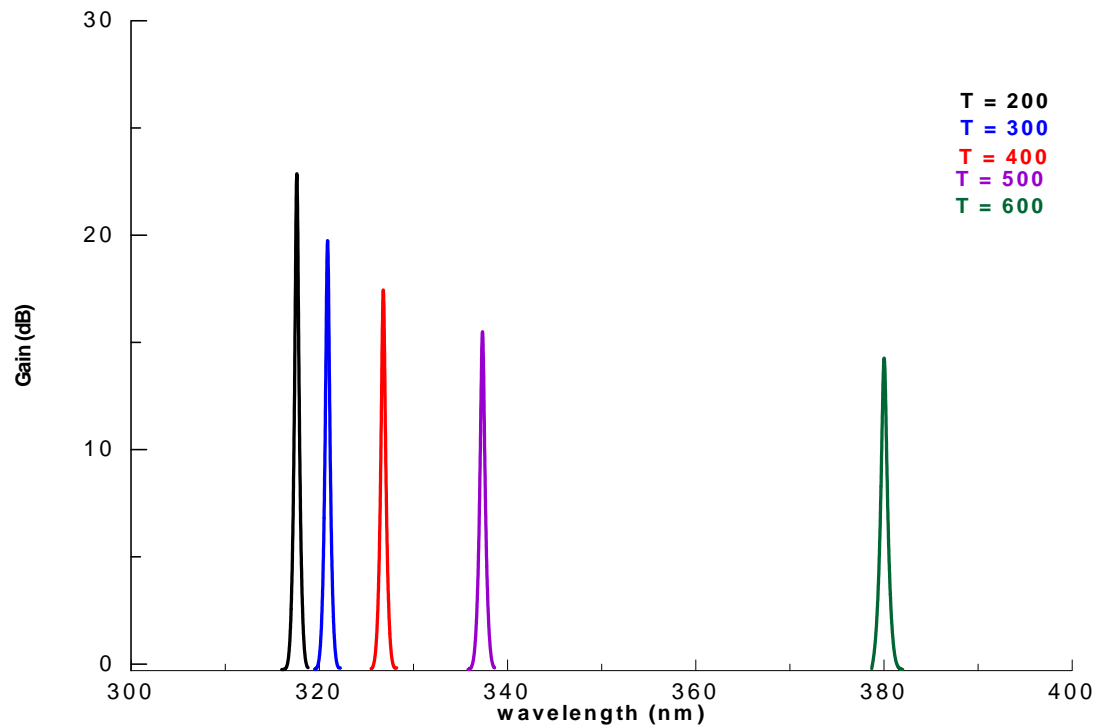


Fig. (5): small signal gain versus wavelength for temperatures ($T = 200, 300, 400, 500$ and 600).

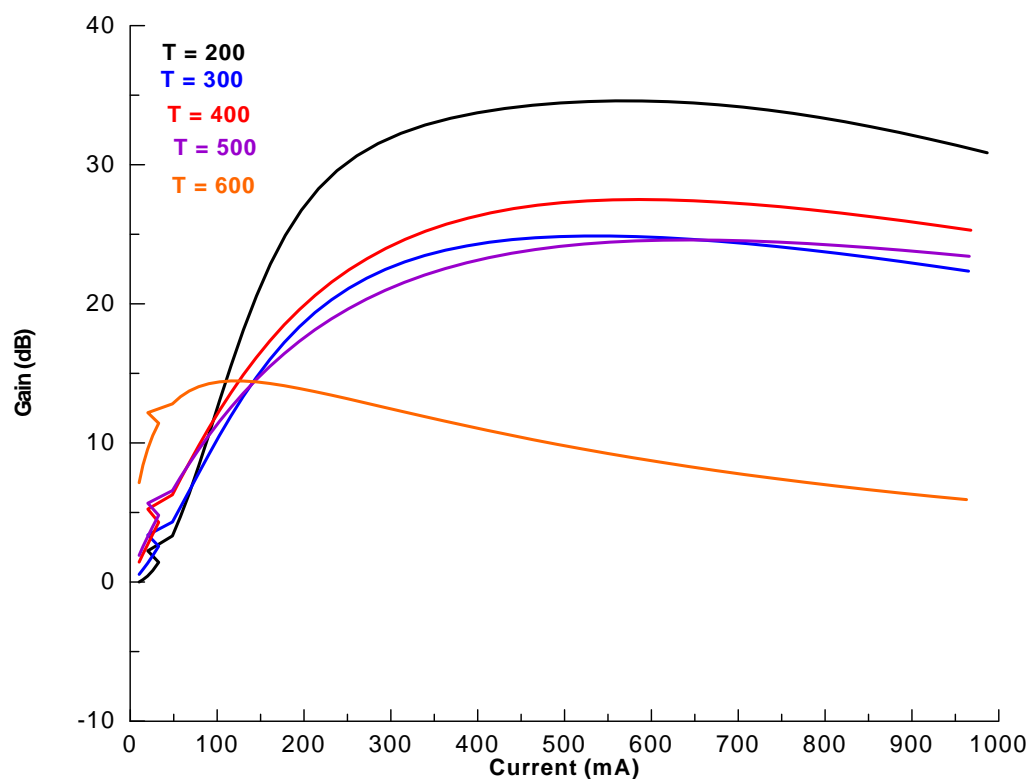


Fig. (6): small signal gain versus current for temperatures ($T = 200, 300, 400, 500$ and 600).

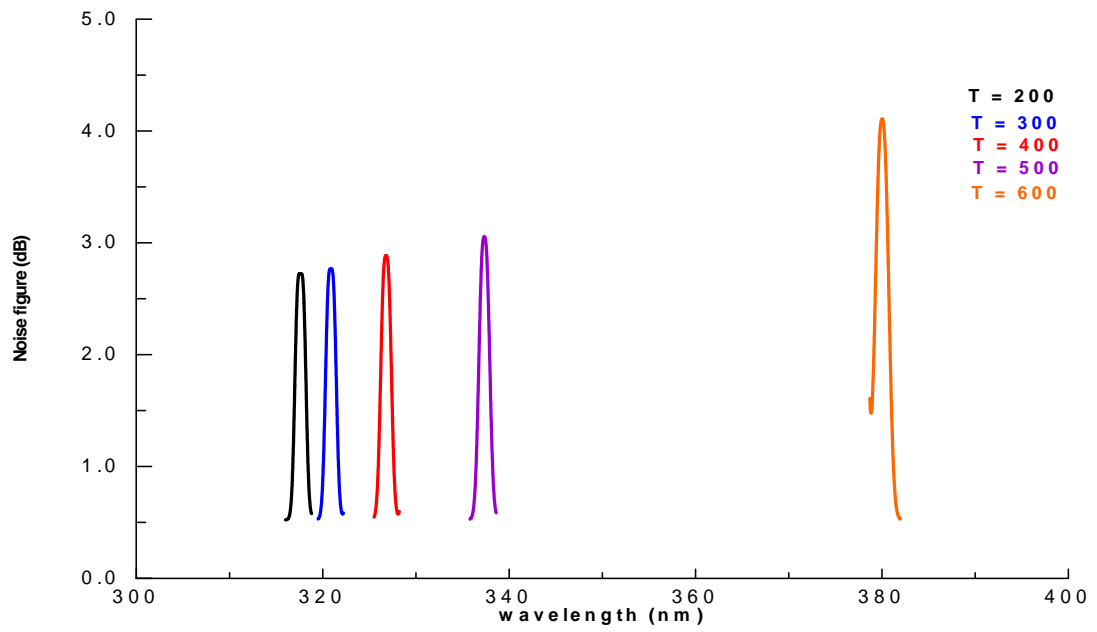


Fig. (7): Noise figure versus wavelength for temperatures ($T = 200, 300, 400, 500$ and 600).

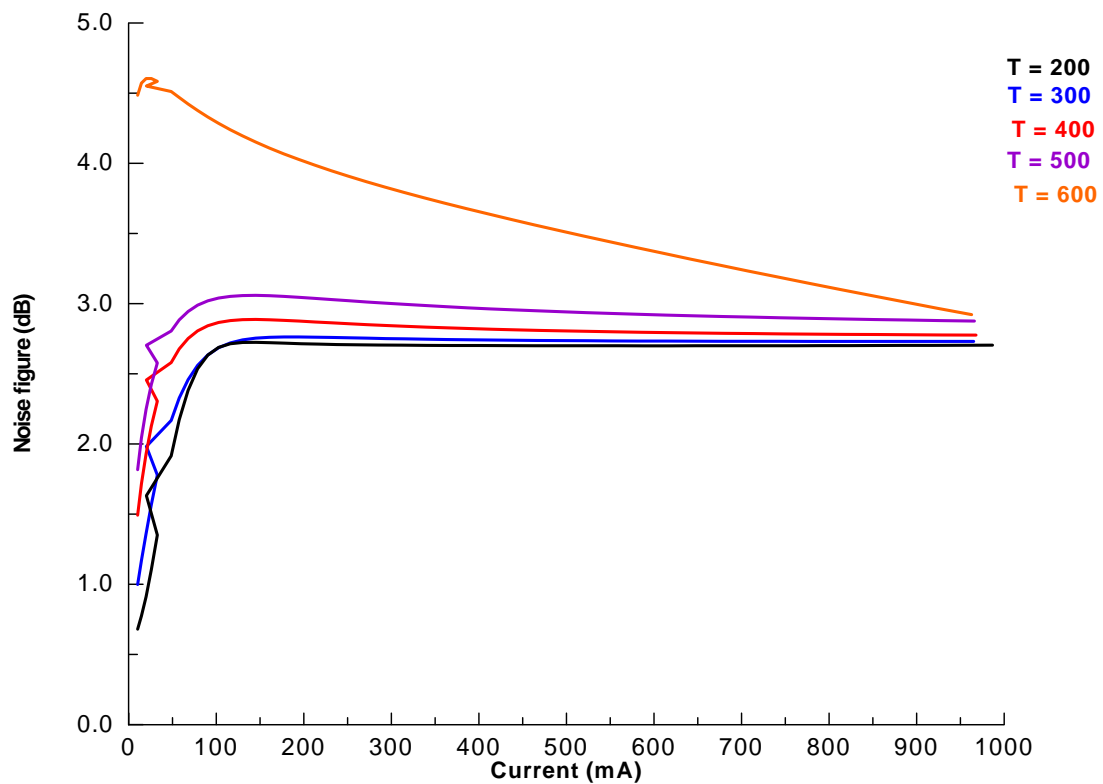


Fig. (8): Noise figure versus current for temperatures ($T = 200, 300, 400, 500$ and 600).

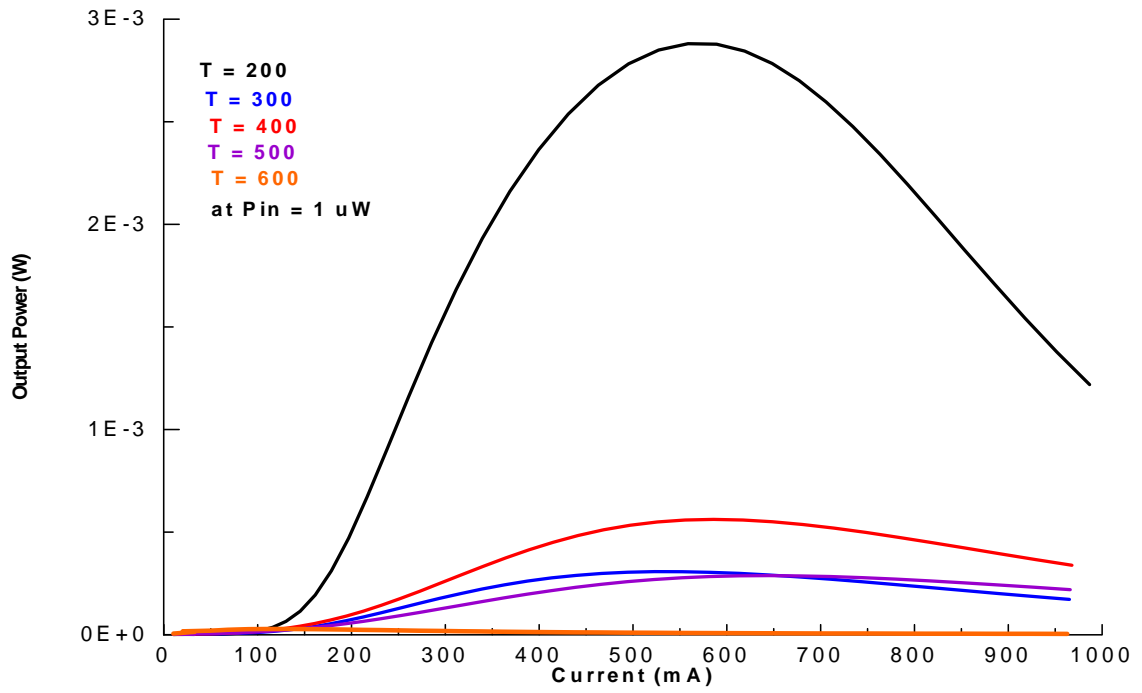


Fig. (9): Output power versus current for temperatures ($T = 200, 300, 400, 500$ and 600) at $P_{in} = 1 \mu W$.